JPET Fast Forward. Published on April 28, 2020 as DOI: 10.1124/jpet.120.265892
This article has not been copyedited and formatted. The final version may differ from this version.

Comparative Pharmacokinetics of Δ^9-Tetrahydrocannabinol in Adolescent and Adult Male Mice¶#

Alexa Torrens[1]*, Valentina Vozella[1]*, Hannah Huff[2], Brandon McNeil[1]
Faizy Ahmed[1], Andrea Ghidini[1,3], Stephen V. Mahler[4], Marilyn A. Huestis[5],
Aditi Das[2], Daniele Piomelli[1,6,7]

[1]Department and Anatomy and Neurobiology
University of California, Irvine, CA 92697-4625, USA

[2]Department of Chemistry
University of Illinois at Urbana-Champaign, Urbana, IL, 61802

[3]Dipartimento di Scienza degli Alimenti e del Farmaco,
Università degli Studi di Parma, Parma, I-43124 Italy

[4]Department of Neurobiology and Behavior,
University of California, Irvine, CA 92697-4625, USA

[5]Institute of Emerging Health Professions,
Thomas Jefferson University, Philadelphia, PA 19107, USA

[6]Department of Biological Chemistry
University of California, Irvine, CA 92697-4625, USA

[7]Department of Pharmaceutical Sciences
University of California, Irvine, CA 92697-4625, USA

*Equal contribution

JPET Fast Forward. Published on April 28, 2020 as DOI: 10.1124/jpet.120.265892
This article has not been copyedited and formatted. The final version may differ from this version.

A. Pharmacokinetics of Δ^9-THC in Adolescent and Adult Mice

B. Correspondence should be addressed to:

Daniele Piomelli

Anatomy & Neurobiology

Gillespie Neuroscience Res. Facility

837 Health Sciences Rd.

Room 3101

Irvine, CA 92697

piomelli@hs.uci.edu

C. Text pages: 32; Tables: 4; Figures: 6; References: 40; Abstract: 222; Introduction: 553; Discussion: 1413.

D. ATB-binding cassette transporter, ABC-transporter; blood-brain barrier, BBB; breast cancer resistance protein, *Abcg2*; claudin-5, Cldn5; cytochrome P_{450}, CYP_{450}; elimination rate constant, λ_z; electrospray-ionization, ESI; 11-hydroxy-Δ^9-THC, 11-OH-THC; internal standard, ISTD; clearance, CL; liquid-chromatography/tandem mass spectrometry, LC-MS/MS; maximum concentration, C_{max}; multiple reaction monitoring, MRM; 11-nor-9-carboxy-Δ^9-THC, 11-COOH-THC; P-glycoprotein, *Abcb1*; pharmacokinetics, PK; Δ^9-tetrahydrocannabinol, Δ^9-THC; time maximum concentration reached, T_{max}; volume of distribution, V_D; white adipose tissue, WAT.

E. Neuropharmacology

JPET Fast Forward. Published on April 28, 2020 as DOI: 10.1124/jpet.120.265892
This article has not been copyedited and formatted. The final version may differ from this version.

ABSTRACT

We investigated the pharmacokinetic properties of Δ^9-tetrahydrocannabinol (Δ^9-THC), the main psychoactive constituent of cannabis, in adolescent and adult male mice. The drug was administered at logarithmically ascending doses (0.5, 1.6 and 5 mg/kg, intraperitoneal) to pubertal adolescent (37-day old) and adult (70-day old) mice. Δ^9-THC and its first-pass metabolites – 11-hydroxy-Δ^9-THC (11-OH-THC) and 11-nor-9-carboxy-Δ^9-THC (11-COOH-THC) – were quantified in plasma, brain and white adipose tissue (WAT) using a validated isotope-dilution liquid chromatography/tandem mass spectrometry assay. Δ^9-THC (5 mg/kg) reached 50% higher circulating concentration in adolescent than in adult mice. A similar age-dependent difference was observed in WAT. Conversely, 40% to 60% lower brain concentrations and brain-to-plasma ratios for Δ^9-THC and 50% to 70% higher brain concentrations for Δ^9-THC metabolites were measured in adolescent relative to adult animals. Liver microsomes from adolescent mice converted Δ^9-THC into 11-COOH-THC twice as fast as adult microsomes. Moreover, the brain of adolescent mice contained higher mRNA levels of the multi-drug transporter *Abcg2*, which may extrude Δ^9-THC from the brain, and higher mRNA levels of claudin-5, a protein that contributes to blood-brain barrier integrity. Finally, administration of Δ^9-THC (5 mg/kg) reduced spontaneous locomotor activity in adult, but not adolescent animals. The results reveal the existence of multiple differences in the distribution and metabolism of Δ^9-THC between adolescent and adult male mice, which might influence the pharmacological response to the drug.

JPET Fast Forward. Published on April 28, 2020 as DOI: 10.1124/jpet.120.265892
This article has not been copyedited and formatted. The final version may differ from this version.

SIGNIFICANCE STATEMENT

Animal studies suggest that adolescent exposure to Δ^9-tetrahydrocannabinol (Δ^9-THC), the intoxicating constituent of cannabis, causes persistent changes in brain function. These studies generally overlooked the impact that age-dependent changes in the distribution and metabolism of the drug might exert on its pharmacological effects. This report provides a comparative analysis of the pharmacokinetic properties of Δ^9-THC in adolescent and adult male mice, and outlines multiple functionally significant dissimilarities in the distribution and metabolism of Δ^9-THC between these two age groups.

JPET Fast Forward. Published on April 28, 2020 as DOI: 10.1124/jpet.120.265892
This article has not been copyedited and formatted. The final version may differ from this version.

INTRODUCTION

As with other psychoactive drugs, cannabis use typically starts in early teenage years and progressively increases throughout adolescence: in 2018, 35.7% of 12th graders in American schools tried the drug at least once (Johnston et al., 2019). Teenagers use cannabis more than any other recreational substance and many also experiment with novel synthetic cannabinoids (Johnston et al., 2019). Furthermore, the growing diffusion of medical cannabis-derived products – for example, for childhood epilepsy and autism symptoms – is exposing new groups of young people to the drug. These trends are of particular concern within a social context in which broadening acceptance and legislative changes fuel financial interests that can potentially override public health and safety concerns (Piomelli, 2015; Kalant, 2015).

Brain networks controlling human emotion and cognition are still actively developing during adolescence (Spear, 2000; Steinberg, 2005), and this plastic state makes them particularly sensitive to disruption by cannabinoid agents and other insults (Lubman et al., 2015). Indeed, there is an overall consensus across epidemiological surveys that adolescent-onset use of cannabis is associated with impairments in cognition and affect that continue into adulthood even after use of the drug has stopped (Schweinsburg et al., 2008). Supporting a causal link between cannabis use and changes in brain function, studies showed that exposing adolescent mice and rats to the psychotropic constituent of cannabis, Δ^9-tetrahydrocannabinol (Δ^9-THC), or one of its synthetic mimics causes persistent dysregulations in affect, memory and reward-seeking behavior (for review, see Rubino and Parolaro, 2016). Despite their mechanistic value, these animal experiments generally discounted the possible pharmacodynamic consequences of age-related changes in the absorption, distribution and metabolism of Δ^9-THC. Such changes are to be expected, however. Indeed, the scientific literature offers substantial evidence for developmental regulation of xenobiotic metabolism *via* the hepatic cytochrome P_{450} (CYP_{450}) system (Sadler et al., 2016), plasma protein binding activity (Sethi et al., 2016) and blood-brain barrier (BBB) function (Goodall et al., 2018). These parameters are critical to the disposition of

JPET Fast Forward. Published on April 28, 2020 as DOI: 10.1124/jpet.120.265892
This article has not been copyedited and formatted. The final version may differ from this version.

Δ^9-THC, a hydrophobic substance that avidly binds to serum albumin (Wahlqvist et al., 1970; Fanali et al., 2011), undergoes extensive first-pass liver metabolism (for review, see Huestis, 2007; Lucas et al., 2018) (Supplementary Fig. 1), and must enter the brain to produce its characteristic intoxicating effects.

To fill this knowledge gap, in the present study we carried out a comparative analysis of the pharmacokinetic (PK) properties of Δ^9-THC in pubertal adolescent (37 day-old) and adult (70 day-old) male mice. We administered the drug by intraperitoneal (IP) injection, the most common route used in animal models, and quantified Δ^9-THC and its main CYP_{450} metabolites [11-hydroxy-Δ^9-THC (11-OH-THC) and 11-nor-9-carboxy-Δ^9-THC (11-COOH-THC)] in plasma, brain and white adipose tissue (WAT) using an isotope-dilution liquid chromatography/tandem mass spectrometry (LC-MS/MS) assay validated following Food and Drug Administration guidelines (Vozella et al., 2019). Additionally, we measured *(i)* the conversion of Δ^9-THC into 11-OH-THC and 11-COOH-THC by liver microsomal fractions; *(ii)* the transcription in brain of multi-drug transporters, *Abcb1* and *Abcg2*, which are thought to extrude Δ^9-THC from the brain (Leishmann et al., 2018), and of claudin-5, a tight-junction protein involved in BBB integrity (Greene et al., 2019); and *(iii)* the effects of Δ^9-THC (5 mg/kg) on spontaneous locomotor activity. The results reveal the existence of significant dissimilarities in the distribution and metabolism of Δ^9-THC between adolescent and adult mice, which might influence wide-ranging pharmacological responses to the drug.

JPET Fast Forward. Published on April 28, 2020 as DOI: 10.1124/jpet.120.265892
This article has not been copyedited and formatted. The final version may differ from this version.

MATERIALS AND METHODS

Chemicals and solvents

[$^2H_3$]-Δ^9-THC, [$^2H_3$]-11-OH-THC, and [$^2H_3$]-11-COOH-THC were purchased from Cerilliant (Round Rock, TX). Δ^9-THC was from Cayman Chemicals (Ann Arbor, MI). All analytical solvents were of the highest grade, and were obtained from Honeywell (Muskegon, MI) or Sigma-Aldrich (Saint Louis, MO). Formic acid was from Thermo Fisher (Houston, TX).

Animals

Adolescent (post-natal day, PND, at arrival: 25-30, 15-20 g) and adult (PND ≥ 60, 20-25 g) male C57BL/6 mice were obtained from Charles River (Wilmington, MA). They were housed in groups of 4 and were allowed to acclimate for at least 3 days before experiments. Housing rooms were maintained on a 12-h light/12-h dark cycle (lights on at 6:30 AM) under controlled conditions of temperature (20 ± 2°C) and relative humidity (55–60%). Food and water were available ad libitum. All procedures were approved (protocol number AUP 18-053) by the Institutional Animal Care and Use Committee at the University of California, Irvine, and carried out in strict accordance with the National Institutes of Health guidelines for the care and use of experimental animals.

Pharmacokinetic experiments

We dissolved Δ^9-THC (Cayman) in a vehicle consisting of Tween80/saline (5:95, v/v) (Burston et al., 2010) and administered it at ascending dosages (0.5, 1.6 or 5 mg/kg) by intraperitoneal (IP) injection to pubertal adolescent (PND 37) or adult (PND 70) mice in an injection volume of 10 mL/kg. Mice were anesthetized with isoflurane at various time points (15, 30, 60, 120, 240 and 480 min) after injection of one of the Δ^9-THC doses, blood (approximately 0.5 mL) was collected by cardiac puncture into ethylenediamine-tetraacetic acid (EDTA)-rinsed syringes and transferred into 1 mL polypropylene plastic tubes containing spray-coated potassium-EDTA (K_2-EDTA).

Plasma was prepared by centrifugation at 1450×*g* at 4°C for 15 min, and transferred into polypropylene tubes, which were immediately frozen and stored at -80ºC. Analyses were conducted within one week or less of sample collection. The animals were euthanized by decapitation and their brains were quickly removed and bisected mid-sagittally on an ice-cold glass plate. Epididymal white adipose tissue (WAT) was collected and rinsed in cold saline. All tissue samples were frozen on dry ice and stored at -80°C until analyses.

Sample preparation

Plasma (0.1 mL) was transferred into 8 mL glass vials (Thermo Fisher) and proteins were precipitated by addition of 0.5 mL ice-cold acetonitrile containing 1% formic acid and the following internal standards (ISTD): [$^2H_3$]-Δ^9-THC, [$^2H_3$]-11-OH-THC, and [$^2H_3$]-11-COOH-THC, 50 pmol each. Half-brains were homogenized in 5 mL ice-cold acetonitrile containing 1% formic acid. The homogenates (1 mL) were collected and spiked with 50 pmol ISTD. Epididymal WAT (20-30 mg) was homogenized in 1 mL of ice-cold acetonitrile containing 1% formic acid and 50 pmol ISTD. Plasma, brain, and WAT samples were stirred vigorously for 30 s and centrifuged at 2800×*g* at 4°C for 15 min. After centrifugation, the supernatants were loaded onto Captiva-Enhanced Matrix Removal (EMR)-Lipid cartridges (Agilent Technologies, Santa Clara, CA) and eluted under vacuum (3–5 mmHg). For brain and WAT fractionation, EMR cartridges were pre-washed with water/acetonitrile (1:4, v/v). No pretreatment was necessary for plasma fractionation. Tissue pellets were rinsed with water/acetonitrile (1:4, v/v; 0.2 mL), stirred for 30 s, and centrifuged at 2800×*g* at 4°C for 15 min. The supernatants were collected, transferred onto EMR cartridges, eluted, and pooled with the first eluate. The cartridges were washed again with water/acetonitrile (1:4, v/v; 0.2 mL), and vacuum pressure was increased gradually to 10 mmHg to ensure maximal analyte recovery. Eluates were dried under N_2 and reconstituted in 0.1 mL of methanol containing

JPET Fast Forward. Published on April 28, 2020 as DOI: 10.1124/jpet.120.265892
This article has not been copyedited and formatted. The final version may differ from this version.

0.1% formic acid. Samples were transferred to deactivated glass inserts (0.2 mL) placed inside amber glass vials (2 mL; Agilent Technologies).

Liquid chromatography/tandem mass spectrometry (LC-MS/MS) analyses

A representative LC-MS/MS tracing is illustrated in Supplementary Figure 2. LC separations were carried out using a 1200 series LC system (Agilent Technologies), consisting of a binary pump, degasser, thermostated autosampler and column compartment coupled to a 6410B triple quadrupole mass spectrometric detector (MSD; Agilent Technologies). Analytes were separated on an Eclipse XDB C18 column (1.8 μm, 3.0 × 50.0 mm; Agilent Technologies). The mobile phase consisted of water containing 0.1% formic acid as solvent A and methanol containing 0.1% formic acid as solvent B. The flow rate was 1.0 mL/min. The gradient conditions were as follows: starting 75% B to 89% B in 3.0 min, changed to 95% B at 3.01 min, and maintained till 4.5 min to remove any strongly retained materials from the column. Equilibration time was 2.5 min. The column temperature was maintained at 40°C and the autosampler at 9°C. The total analysis time, including re-equilibrium, was 7 min. The injection volume was 5 μL. To prevent carry over, the needle was washed in the autosampler port for 30 s before each injection using a wash solution consisting of 10% acetone in water/methanol/isopropanol/acetonitrile (1:1:1:1, v/v). The MS was operated in the positive electrospray ionization (ESI) mode, and analytes were quantified by multiple reaction monitoring (MRM) of the following transitions: Δ^9-THC 315.2 > 193.0 *m/z*, [$^2H_3$]-Δ^9-THC 318.2 > 196.1 *m/z*, 11-OH-THC 331.2 > 313.1 *m/z*, [$^2H_3$]-11-OH-THC 334.2 > 316.1 *m/z*, 11-COOH-THC 345.2 > 299.2 *m/z*, [$^2H_3$]-11-COOH-THC 348.2 > 302.2 *m/z*. In select experiments, we further verified the identity of Δ^9-THC by monitoring the transition 315.2 > 135.0 *m/z* (Supplementary Fig. 2). The capillary voltage was set at 3500 V. The source temperature was 300°C and gas flow was set at 12.0 L/min. Nebulizer pressure was set at 40 psi. Collision energy and fragmentation voltage were set for each analyte as reported (Vozella et al., 2019).

The MassHunter software (Agilent Technologies) was used for instrument control, data acquisition, and data analysis.

Liver microsome preparation

Microsomes were prepared as described (McDougle et al., 2014) with minor modifications. Briefly, mouse livers were weighed and homogenized in extraction buffer (20%, w/v; 10 mM Tris pH 7.5, 250 mM sucrose, 1 mM phenylmethylsulfonyl fluoride, Protease Inhibitor Cocktail, Nacalai Tesque, Kyoto, Japan, cat no.: 04080-11). The homogenates were centrifuged at 3000×*g* at 4°C for 20 min. Supernatants were collected and centrifuged twice for 20 min at 10,000×*g* at 4°C. The supernatants from the second centrifugation were centrifuged again for 90 min at 100,000×*g* at 4°C. The microsome pellets were resuspended in 0.5 mL buffer (50 mM Tris pH 7.5, 20% glycerol, 1 mM dithiothreitol, 1 mM EDTA). Protein concentrations were measured using the bicinchoninic acid (BCA) assay.

Δ^9-THC metabolism in liver microsomes

Microsomes (1 μg protein) were combined in a solution of potassium phosphate (0.1 M, pH 7.4) and rat cytochrome P_{450} reductase (0.2 μM). After a 5 min, 37°C preincubation with Δ^9-THC (40 μM, final concentration of DMSO was 1.2%), reactions were initiated by adding 10 mM NADPH (0.1 mL,1 mM final) and allowed to proceed at 37°C for 30 min, at which point they were quenched with an equal volume of ethyl acetate. Extractions were performed as previously reported (Huff et al., 2019). Briefly, the quenched reactions were vortexed thoroughly, centrifuged for 5 min at 1800×*g* at 4°C, and the organic layers were transferred into clean tubes. Fresh ethyl acetate was added, and the cycle was repeated twice for a total of 3 extractions. After drying down the organic layer in a rotary evaporator, extracts were resuspended in acetonitrile (0.1 mL) and 11-OH-THC and 11-COOH-THC were quantified by LC-MS/MS using a 5500 QTRAP LC-MS/MS system

JPET Fast Forward. Published on April 28, 2020 as DOI: 10.1124/jpet.120.265892
This article has not been copyedited and formatted. The final version may differ from this version.

(Sciex, Framingham, MA) connected to a 1200 series LC system (Agilent Technologies, Santa Clara, CA), which included a degasser, an autosampler, and a binary pump. The LC separation was performed on an Agilent Eclipse XDB-C18 column (4.6 × 150 mm, 5 µm) with mobile phase A (0.1% formic acid in water) and mobile phase B (0.1% formic acid in acetonitrile). The flow rate was 0.4 mL/min and the linear gradient was as follows: 0-2 min, 90% A; 10-23 min, 5% A; 24-31 min, 90% A. The autosampler was set at 5°C and the injection volume was 10 µL. Mass spectra were acquired under positive (ion spray voltage 5500 V) ESI. The source temperature was 450°C. The curtain gas, ion source gas 1, and ion source gas 2 were 32, 65, and 50 psi, respectively. MRM was used for quantitation: Δ^9-THC 315.2 > 193.0 *m/z*; 11-OH-THC 331.2 > 331.2 *m/z*; 11-COOH-THC 345.2 > 327.2 *m/z*. Internal standard was [$^2H_9$]-Δ^9-THC (324.2 > 202.1 *m/z*). Software Analyst 1.6.2 was used for data acquisition and analysis.

RT-PCR analyses

Total RNA was prepared from brain tissue of adolescent (PND 37) and adult (PND 70) male mice using an Ambion PureLink RNA minikit (Life Technologies, Carlsbad, CA) as directed by the supplier. Samples were treated with DNase (PureLink DNase, Life Technologies) and cDNA synthesis was carried out using Applied Biosystems High Capacity cDNA Reverse Transcription Kit (Thermofisher) according to the manufacturer's protocol using purified RNA (2 µg). First-strand cDNA was amplified using the QuantiFast SYBR Green PCR Kit (Qiagen, Hilden, Germany), fluorogenic probes, and oligonucleotide primers. Copy numbers of cDNA targets were quantified at the point during cycling when the PCR product was first detected. Gene-specific primers for mouse ATP-binding cassette (ABC) transporters, P-glycoprotein (*Abcb1*, F: 5'-CCCGGCTCACAGATGATGTT-3' and R: 5'-TTCCAGCCACGGGTAAATCC-3') and breast cancer resistance protein (*Abcg2,* F: 5'-CAGCAAGGAAAGATCCAAAGGG-3' and R: 5'-CACAACGTCATCTTGAACCACA-3'), and integral membrane protein, claudin-5 (*Cldn5*, F: 5'-

TGACTGCCTTCCTGGACCACAA-3' and R: 5'-CATACACCTTGCACTGCATGTGC-3'), were purchased from Life Technologies. Quantitative PCR was performed in 96-well PCR plates and run at 95°C for 10 min, followed by 40 cycles, each cycle consisting of 15 s at 95°C and 1 min at 60°C, using a Stratagene Mx 3000P (Agilent). The BestKeeper software (Pfaffl et al., 2004) was used to determine expression stability and geometric mean of different housekeeping genes (*Gapdh* and *Actin-b*). ΔCt values were calculated by subtracting the Ct value of the geometric mean of these housekeeping genes from the Ct value for the genes of interest. The relative quantity of the genes of interest was calculated by the expression 2^-ΔΔCt. Results are reported as fold induction over control.

Motor activity

Animals were habituated to the test cages for 3 days prior to trial. Adult and adolescent mice were injected IP with vehicle (saline, 0.9%) or Δ^9-THC (5 mg/kg) and motor activity was recorded using an automated system (TSE Technical & Scientific Equipment GmbH, Bad Homburg, Germany) starting at 9:00 AM and lasting for 6 h, the first 2 h of activity were analyzed. The system consisted of cages equipped with an activity-detecting frame with 6x2 infrared sensors in the XY-plane (56 mm apart on the long axis, 140 mm apart on the short) and 4 sensors in the Z plane (56 mm apart). The XY plane the recorded horizontal position of the animal and the Z plane detected rearing and jumps (vertical activity). Each sensor consisted of a transmitting and receiving component arranged at right angles. Sensors scanned sequentially at a rate of 56 Hz to determine the coordinates of each animal. Each sensor interruption was registered as a "beam break". The data were analyzed as average number of beam breaks per 30 min.

Analyses of PK data

JPET Fast Forward. Published on April 28, 2020 as DOI: 10.1124/jpet.120.265892
This article has not been copyedited and formatted. The final version may differ from this version.

We analyzed PK data using a non-compartmental model (Gabrielsson and Weiner, 2012). Maximal concentration (C_{max}) and area under the curve (AUC) were measured using GraphPad Prism 8 (La Jolla, CA) and other PK parameters (elimination rate constant (λ_z), clearance (CL), volume of distribution (V_D), and half-life time of elimination ($t_{1/2}$)) were determined as described (Gabrielsson and Weiner, 2012). In regards to CL and V_D calculations, the following equations were used: CL = dose/AUC; $V_D = CL/\lambda_z$. Times at which the maximal concentrations were reached (T_{max}) were determined by visual inspection of averaged data.

Statistical analyses

Data were analyzed using GraphPad Prism 8 by either Student's unpaired *t*-test or two-way analysis of variance (ANOVA) with Bonferroni post hoc analysis. Outliers were determined using Grubbs' outlier test. Differences between groups were considered statistically significant at $P < 0.05$.

RESULTS

Pharmacokinetic profile of Δ^9-THC in mouse plasma

Figure 1A-C shows the plasma PK profiles for Δ^9-THC and its two main first-pass metabolites, 11-OH-THC and 11-COOH-THC, in adult (PND 70) male mice after IP administration of logarithmically ascending doses of Δ^9-THC (0.5, 1.6 or 5 mg/kg). Table 1 reports the peak concentration (C_{max}) in plasma, the area under the curve (AUC), the time at which C_{max} was attained (T_{max}) and the half-life time ($t_{1/2}$) of elimination for each of the three compounds. At the 5 mg/kg dose, Δ^9-THC reached a C_{max} of 631 ± 64 pmol/mL (198 ± 20 ng/mL, mean ± SEM) with a T_{max} of 30 min. Maximal plasma concentrations of 11-OH-THC and 11-COOH-THC were 65 ± 6 pmol/mL and 260 ± 18 pmol/mL, respectively, and were also reached 30 min after injection. Plasma $t_{1/2}$ values for Δ^9-THC were comparable across dosages (109 ± 7 min at 5 mg/kg, 108 ± 18 min at 1.6 mg/kg, and 92 ± 10 min at 0.5 mg/kg). The apparent volume of distribution (V_D) of Δ^9-THC in adult mice, calculated using a non-compartmental pharmacokinetic model (Gabrielsson and Weiner, 2012), was 808 ± 83 mL (λ_z = 0.005 ± 0.0004), and the clearance (CL) was 4.4 ± 0.2 mL/min.

Similar plasma PK profiles were observed in pubertal adolescent (PND 37) mice, with some notable exceptions (Fig. 1D-F and Table 1). At the 5 mg/kg dose, the C_{max} for Δ^9-THC was 76% higher in adolescents than in adults. Moreover, at the 5 and 0.5 mg/kg doses, plasma C_{max} and AUC values for Δ^9-THC metabolites were greater than the corresponding concentrations in adult mice. For example, after injection of 5 mg/kg Δ^9-THC, the C_{max} for 11-COOH-THC was 2.5 times higher in adolescents than in adults (654 ± 22 *vs* 260 ± 18 pmol/mL). At the same dose, the plasma T_{max} for Δ^9-THC occurred earlier in adolescent (15 min) than in adult (30 min) animals, and elimination was faster ($t_{1/2}$ = 75 ± 9 *vs* 109 ± 7 min). The V_D of Δ^9-THC in adolescents was 442 ± 54 mL (λ_z = 0.008 ± 0.001), and the CL was 3.6 ± 0.1 mL/min, and both were lower (P <

0.05) than the corresponding values in adults, providing a possible explanation for the higher peak concentrations of Δ^9-THC in plasma, compared to adults.

Pharmacokinetic profile of Δ^9-THC in brain

The PK profiles of Δ^9-THC and its metabolites in the brain of adult mice are illustrated in Figure 2A-C. Key PK parameters are reported in Table 2. At 5 mg/kg, the C_{max} for Δ^9-THC was 1126 $\pm$ 110 pmol/g, the T_{max} was 120 min and the $t_{1/2}$ of elimination was 119 $\pm$ 9 min. Of note, the brain-to-plasma ratio of Δ^9-THC was relatively low (1.9 $\pm$ 0.4) (Table 3), but consistent with values previously reported in the literature (Watanabe et al., 1980; Spiro et al., 2012). 11-OH-THC and 11-COOH-THC reached C_{max} values of 339 $\pm$ 49 and 89 $\pm$ 6 pmol/g, respectively, both at a T_{max} of 120 min (Table 2). The brain-to-plasma ratios for 11-OH-THC and 11-COOH-THC were 6.4 $\pm$ 0.9 and 0.4 $\pm$ 0.04, respectively (Table 3).

Comparing the data in Figure 2A and Figure 2D show that, at the 5 mg/kg dose, brain C_{max} for Δ^9-THC was 55% higher in adult than in adolescent mice. The AUC was also 38% higher in the older group (Table 2). Conversely, C_{max} and AUC values for Δ^9-THC metabolites were either lower or showed trends to be lower in adult animals. Lastly, the brain-to-plasma ratios for Δ^9-THC and its metabolites were higher in adults than in adolescents (Table 3). In sum, the findings suggest that adolescent mice treated with Δ^9-THC attain lower peak brain concentrations of the non-metabolized drug, but higher brain concentrations of its metabolites, relative to adults. This finding is suggestive of age-dependent changes in the ability of Δ^9-THC and its metabolites to access the brain, and raises the intriguing possibility that the drug might undergo local metabolism within the central nervous system.

Pharmacokinetic profile of Δ^9-THC in WAT

Figure 3 shows the PK profiles of Δ^9-THC and its first-pass metabolites in epididymal WAT. PK parameters are reported in Table 4. In adult mice, injection of 5 mg/kg Δ^9-THC produced a C_{max} of 134 ± 16 nmol/g (1.34 x 10^5 pmol/g) at a T_{max} of 30 min (Fig. 3A). The C_{max} for 11-OH-THC was 2 ± 0.2 nmol/g (at T_{max} 30 min) and the C_{max} for 11-COOH-THC was 0.1 ± 0.01 nmol/g (at T_{max} 120 min) (Fig. 3B, C). Because Δ^9-THC concentrations in WAT remained virtually unchanged for the entire duration of the experiment (8 hours), $t_{1/2}$ values could not be calculated. The WAT-to-plasma ratio for Δ^9-THC was 200.9 ± 7.9, more than 100 times higher than the brain-to-plasma ratio, while the corresponding values for 11-OH-THC and 11-COOH-THC were 29.7 ± 3.8 and 0.4 ± 0.02, respectively (Table 3), a striking confirmation that adipose tissue serves as a depot for Δ^9-THC and its metabolites (Kreuz and Axelrod, 1973).

In WAT of adolescent mice, C_{max} and AUC values for Δ^9-THC were 81% and 61% higher, respectively, than in adults at the 5 mg/kg dose. The C_{max} for 11-COOH-THC was greater in adolescents than in adults at 5 mg/kg, whereas no statistically detectable differences were seen with 11-COOH-THC at lower Δ^9-THC doses or with 11-OH-THC at any Δ^9-THC dose. Inconsistent variations were observed in T_{max}, which, depending on dose and analyte, could be higher, lower or unchanged between the two age groups (Table 4). Of note, the WAT-to-plasma ratio for Δ^9-THC was comparable in younger and older animals, whereas lower ratios were seen in the former group for both 11-OH-THC and 11-COOH-THC (Table 3). Overall, the results are indicative of a more pronounced accumulation of Δ^9-THC per unit weight of WAT in adolescent mice, compared to adults.

Δ^9-THC metabolism in liver microsomes

The different plasma profiles of 11-COOH-THC in adolescent and adult mice raise the possibility that Δ^9-THC may undergo age-related changes in first-pass metabolism (Fig. 1 and Table 1). To test this, we measured the sequential transformation of Δ^9-THC into 11-OH-THC and 11-COOH-

JPET Fast Forward. Published on April 28, 2020 as DOI: 10.1124/jpet.120.265892
This article has not been copyedited and formatted. The final version may differ from this version.

THC (Supplementary Fig. 1) by liver microsomes. In microsomal preparations from adolescent mice, Δ^9-THC was converted into 11-COOH-THC at a rate of 0.012 ± 0.003 pmol/min/mg, which was approximately twice as rapid as the rate measured in adult microsomes (0.006 ± 0.002 pmol/min/mg) (Fig. 4A). By contrast, the biotransformation of Δ^9-THC into 11-OH-THC was somewhat slower in adolescents compared to adults (adolescents: 1.5 ± 0.19 pmol/min/mg; adults: 1.9 ± 0.05 pmol/min/mg) (Fig. 4B). These findings are consistent with the hypothesis that adolescent mice metabolize Δ^9-THC into 11-COOH-THC more effectively than adults do.

ABC-transporter and claudin-5 mRNA levels in brain

The brain-to-plasma ratio for Δ^9-THC was lower in adolescent mice (Table 3), suggesting that the ability of the drug to access the brain may change with age. To begin testing this hypothesis, we quantified mRNA levels of breast cancer resistance protein (*Abcg2*) and P-glycoprotein (*Abcb1*), two ATP-binding cassette (ABC) transporters present that are thought to extrude Δ^9-THC across the BBB (Spiro et al., 2012). Extracts of adolescent brain tissue contained $P < 0.5$ higher levels of *Abcg2* transcript, compared to adult tissue (Fig 5A). By contrast, *Abcb1* mRNA levels were similar in the two age groups (Fig. 5B). We also measured transcription of claudin-5 (*Cldn5*), a tight junction protein that contributes to BBB structure (Nitta et al., 2003), and found that its mRNA levels were $P < 0.5$ higher in adolescent than in adult brain (Fig. 5C). Thus, alterations in the expression of structural and functional constituents of the BBB might account for the lower Δ^9-THC concentrations observed in the brain of adolescent mice.

Motor effects of Δ^9-THC in adolescent and adult mice

A comparative pharmacodynamic evaluation of adolescent versus adult mice is beyond the scope of the present study. However, a testable prediction from the PK data presented above is that adolescents might be less sensitive than adults to the effects of Δ^9-THC. To test this, we

JPET Fast Forward. Published on April 28, 2020 as DOI: 10.1124/jpet.120.265892
This article has not been copyedited and formatted. The final version may differ from this version.

administered vehicle (saline, 0.9%) or Δ^9-THC (5 mg/kg) to groups of adolescent and adult male mice (n = 10 per group) and measured locomotor activity in a familiar environment for the following 2 hours. The results, illustrated in Fig. 6, suggest that Δ^9-THC caused a rapid and short-lived decrease in locomotor activity in adult, but not adolescent male mice. This finding supports the possibility, suggested by our PK studies, that the central nervous system of adolescent mice is partially protected from the pharmacological effects of Δ^9-THC.

JPET Fast Forward. Published on April 28, 2020 as DOI: 10.1124/jpet.120.265892
This article has not been copyedited and formatted. The final version may differ from this version.

DISCUSSION

The long-term consequences of Δ^9-THC exposure during adolescence have been the object of many animal studies (for a recent review, see Rubino and Parolaro, 2016), but the question of whether the PK properties of the drug might change in the transition from adolescence to adulthood was not systematically addressed. Filling this gap is important, however, to understand whether age-dependent changes in the pharmacological response to Δ^9-THC may result solely from developmental alterations in endocannabinoid signaling – for example, in the number of cannabinoid receptors or intrinsic activity of the endocannabinoid system – or might also involve adjustments in the distribution, biotransformation and elimination of the drug. In the present report, we assessed the PK behavior of Δ^9-THC and its two primary first-pass metabolites, 11-OH-THC and 11-COOH-THC, following IP administration in adolescent and adult male mice. The results identify multiple dissimilarities in the distribution and metabolism of Δ^9-THC between the two age groups, including potentially relevant differences in peak drug concentrations in plasma and brain, brain-to-plasma ratio, and CYP_{450}-mediated metabolism. These results may have wide-ranging implications for the interpretation of mouse adolescent Δ^9-THC exposure studies.

In the present report, we selected the IP route of administration for two reasons: first, it's the route most frequently used in animal studies and, second, it represents a realistic compromise between experimental feasibility and human relevance. In fact, our results show that IP injection results in substantial and reproducible tissue concentrations of Δ^9-THC in both adolescent and adult mice, and produces peaks in plasma concentrations that are quantitatively comparable to those observed in adult non-medical cannabis smokers (Huestis, 2007). For example, the data reported in Table 1 show that the C_{max} for Δ^9-THC after administration of a 5 mg/kg dose in adult mice (198 $\pm$ 20 ng/mL at 30 min) is similar to the C_{max} measured in the blood of persons who smoked one cannabis cigarette containing ≈34 mg of Δ^9-THC (162 $\pm$ 34 ng/mL at ≈ 8 min) (Huestis and Cone, 2004). Such exposure levels are known to be associated with psychotropic activity in humans

(Huestis and Cone, 2004; Cooper and Haney, 2009) as well as in rodents (Pertwee, 2008) and, in the present study, yielded micromolar concentrations of Δ^9-THC in the brain (1126 $\pm$ 110 pmol/g, $\approx$ 1.1 μM), which are likely to fully engage cannabinoid receptors (Pertwee, 2008).

At the 5 mg/kg dose, the peak plasma concentrations (C_{max}) of Δ^9-THC, 11-OH-THC and 11-COOH-THC were all substantially greater in adolescent than in adult mice (Table 1): Δ^9-THC C_{max} was 76% higher, 11-OH-THC 83% higher, and 11-COOH-THC 152% higher. The AUC for 11-COOH-THC was almost twice as large in adolescents as it was in adults (Table 1). Higher C_{max} and AUC values may be consequent to a weaker diversion toward WAT, whose total mass rises as mice become adults, as also suggested by the lower V_D measured in the adolescent group. Irrespective of its origin, greater Δ^9-THC availability might account for the higher 11-OH-THC and 11-COOH-THC concentrations measured in adolescent plasma. Two findings suggest, however, that accrued metabolism might also contribute. First, adolescents eliminated Δ^9-THC at a faster rate than adults did: the plasma $t_{1/2}$ was shorter in the younger group. Second, experiments with liver microsomes – where the majority of Δ^9-THC biotransformation is thought to occur (Christensen et al., 1971; Agurell et al., 1986; Watanabe et al.,1993) – show that the conversion of Δ^9-THC into the inactive metabolite 11-COOH-THC was faster in adolescents (Fig. 5), a result consistent with the known trajectory of CYP_{450} expression in the developing liver (Sadler et al., 2016).

Since plasma concentrations of Δ^9-THC were higher in adolescent than in adult mice, we expected to find a parallel dissimilarity in the brain. This prediction turned out to be incorrect. In fact, C_{max}, AUC and brain-to-plasma ratio for Δ^9-THC (5 mg/kg) were substantially lower in adolescent animals (Tables 2 and 3). The brain-to-plasma ratio for Δ^9-THC was 1.9 $\pm$ 0.4 in adults, which is consistent with values reported in the literature (Watanabe et al., 1980; Spiro et al., 2012), but only 0.8 $\pm$ 0.1 in adolescents. Similarly, the brain C_{max} for Δ^9-THC was 1126$\pm$ 110 pmol/g in adults

JPET Fast Forward. Published on April 28, 2020 as DOI: 10.1124/jpet.120.265892
This article has not been copyedited and formatted. The final version may differ from this version.

and 725 ± 60 pmol/g in adolescents. Supporting these results, pharmacological experiments showed that Δ^9-THC (5 mg/kg) lowered spontaneous locomotor activity in adult, but not adolescent mice (Fig. 6). These findings raised the possibility that mechanisms might exist in adolescents which limit the entry of Δ^9-THC into the central nervous system. As an initial test of this idea, we quantified mRNA levels of two multi-drug ABC transporters, *Abcb1* and *Abcg2*, which were implicated in the removal of Δ^9-THC from brain parenchyma (Spiro et al., 2012). We found that the transcription of *Abcg2*, but not *Abcb1*, was significantly higher in adolescent compared to adult mice (Fig. 5). A similar difference was seen with claudin-5, a protein that is involved in gap junction structure and BBB function (Nitta et al., 2003) and is down-regulated in adult mice following a single administration of Δ^9-THC (3 mg/kg, IP) (Leishmann et al., 2018). Thus, developmental alterations in *Abcg2* and *Cldn5* transcription, and associated changes in blood/brain transfer function, might contribute to the differences in brain Δ^9-THC concentration and pharmacodynamic response observed between adolescent and adult mice. Even though the brain access of Δ^9-THC is detectably lower in adolescent than adult mice, the concentrations of Δ^9-THC metabolites in the brain showed an opposite trend. For example, at the 1.58 and 5 mg/kg doses of Δ^9-THC, 11-COOH-THC levels were 40-70% higher in adolescents than in adults. Potential explanations for this intriguing finding might be the existence of age-dependent changes in either the transport of Δ^9-THC metabolites across the BBB, and/or the metabolism of Δ^9-THC in brain tissue. These explanations are non-exclusive, and testing them will require additional experimentation.

The role of WAT as a reservoir for Δ^9-THC is well established in the literature (Kreuz and Axelrod, 1973; Rawitch et al., 1979; Johansson et al., 1989). Adipose cells can store this hydrophobic substance for weeks after a single injection (Kreuz and Axelrod, 1973) and can release it into the bloodstream when stimulated by lipolytic signals such as fasting or exercise (Gunasekaran et al., 2009; Wong et al., 2013). Consistent with those data, we found that Δ^9-THC (5 mg/kg) reached

sub-millimolar concentrations in WAT, and that such levels remained virtually unchanged for the following 8 hours (Fig. 4). Of note, the PK profile for Δ^9-THC (5 mg/kg) in WAT displayed a unique bimodal shape that distinguished it from plasma and brain (Fig. 4). This might be due to the close anatomical proximity between injection sites in the peritoneum and epididymal fat depots. It is possible, but remains to be demonstrated, that the first peak results from the direct diffusion of Δ^9-THC from the peritoneal cavity into WAT, whereas the second occurs after the drug has entered the bloodstream. We noted several additional differences between adolescent and adult animals in the PK behavior of Δ^9-THC in WAT. For example, depending upon the dose, T_{max} could be longer, earlier or unchanged across age groups (Table 4). Despite these discrepancies, whose interpretation is unclear, the overall results are indicative of a greater accumulation of Δ^9-THC and its metabolites per unit weight of adolescent WAT.

The present report has several limitations, two of which are especially noteworthy. First, our experiments were restricted to male animals and did not address possible sexual dimorphisms in the PK properties of Δ^9-THC. Previous research demonstrated the existence of sex-dependent differences in the biotransformation of Δ^9-THC into 11-OH-THC in adolescent rats (Wiley and Burston, 2014) and similar dimorphisms are also likely to occur in mice. Indeed, a comparative survey of the PK properties of Δ^9-THC in male and female adolescent mice is currently underway in our laboratory. Second, cannabis extracts contain hundreds of chemical constituents, which may impact the PK properties of Δ^9-THC. For instance, cannabidiol may inhibit Δ^9-THC metabolism via CYP3A11 (Stout and Cimino, 2014) while some terpenoids (e.g., borneol) may alter blood-brain barrier permeability (Yin, 2017).

In sum, our experiments reveal the existence of substantial differences in the distribution and metabolism of Δ^9-THC between adolescent and adult male mice — a result with meaningful implications for the interpretation of studies comparing Δ^9-THC effects in these two age groups. In particular, adolescent animals show higher peak concentrations of Δ^9-THC in circulation, along

with more extensive CYP_{450}-mediated metabolism and reduced entry of the drug into the brain. The developmental variations in Δ^9-THC absorption and metabolism across the lifespan clearly deserve further study in both animal models and humans.

AUTHORSHIP CONTRIBUTIONS

Participated in research design: Piomelli, Torrens, Das, Mahler

Conducted experiments: Torrens, Vozella, Huff, McNeil, Ahmed

Performed data analysis: Torrens, Vozella, Huff, Ghidini

Wrote or contributed to the writing of the manuscript: Piomelli, Torrens, Huestis, Mahler

REFERENCES

Agurell S, Halldin MA, Lindgren JE, Ohlsson AG, Widman MA, Gillespie HA, Hollister L (1986) Pharmacokinetics and metabolism of delta 1-tetrahydrocannabinol and other cannabinoids with emphasis on man. Pharmacological Reviews 38: 21-43.

Burston, JJ, Wiley, JL, Craig, AA, Selley, DE, and Sim-Selley, LJ (2010) Regional enhancement of cannabinoid CB_1 receptor desensitization in female adolescent rats following repeated Δ^9-tetrahydrocannabinol exposure. British Journal of Pharmacology 161: 103-112.

Christensen HD, Freudentha R, Gidley JT, Rosenfeld R, Boegli G, Testino L, Brine DR, Pitt CG, and Wall ME (1971) Activity of Δ^8-and Δ^9-tetrahydrocannabinol and related compounds in the mouse. Science 172: 165-167.

Cooper ZD and Haney M (2009) Comparison of subjective, pharmacokinetic, and physiological effects of marijuana smoked as joints and blunts. Drug and Alcohol Dependence 103: 107-113.

Fanali G, Cao Y, Ascenzi P, Trezza V, Rubino T, Parolaro D, and Fasano M (2011) Binding of δ9-tetrahydrocannabinol and diazepam to human serum albumin. IUBMB Life 63: 446-451.

Gabrielsson J and Weiner D (2012). Non-compartmental analysis. Methods Mol Biol. 929: 377-89.

Goodall EF, Want C, Simpson JE, Baker DJ, Drew DR, Heath PR, Saffrey MJ, Romero IA, and Wharton SB (2018) Age-associated changes in the blood-brain barrier: comparative studies in human and mouse. Neuropathology and Applied Neurobiology 44: 328-340.

Greene C, Hanley N, and Campbell M (2019) Claudin-5: gatekeeper of neurological function. Fluids and Barriers of the CNS 16: 3.

Gunasekaran N, Long LE, Dawson BL, Hansen GH, Richardson DP, Li KM, Arnold JC, and McGregor IS (2009) Reintoxication: the release of fat-stored Δ9-tetrahydrocannabinol (THC) into blood is enhanced by food deprivation or ACTH exposure. British Journal of Pharmacology 158: 1330-1337.

Huestis, MA (2007) Human cannabinoid pharmacokinetics. Chemistry and Biodiversity 4: 1770-1804.

Huestis MA and Cone EJ (2004) Relationship of Δ9-tetrahydrocannabinol concentrations in oral fluid and plasma after controlled administration of smoked cannabis. Journal of Analytical Toxicology 28: 394-399.

Huff HC, Maroutsos D, and Das A (2019) Lipid composition and macromolecular crowding effects on CYP2J2-mediated drug metabolism in nanodiscs. Protein Science 28: 928-940.

Johansson E, Norén K, Sjövall J, and Halldin MM (1989) Determination of Δ1-tetrahydrocannabinol in human fat biopsies from marihuana users by gas chromatography–mass spectrometry. Biomedical Chromatography 3: 35-38.

Johnston LD, Miech RA, O'Malley PM, Bachman JG, Schulenberg JE, and Patrick, ME (2019) Monitoring the Future National Survey Results on Drug Use, 1975-2018: Overview, Key Findings on Adolescent Drug Use. Institute for Social Research.

Kalant H (2015) Cannabis control policy: no rational basis yet for legalization. Clinical Pharmacology and Therapeutics 97: 538-540.

Kreuz DS and Axelrod J (1973) Delta-9-tetrahydrocannabinol: localization in body fat. Science 179: 391-393.

Leishman E, Murphy M, Mackie K, and Bradshaw HB (2018) Δ^9-Tetrahydrocannabinol changes the brain lipidome and transcriptome differentially in the adolescent and the adult. Biochimica et Biophysica Acta (BBA)-Molecular and Cell Biology of Lipids 1863: 479-492.

Lubman DI, Cheetham A, and Yücel M (2015) Cannabis and adolescent brain development. Pharmacology and Therapeutics 148: 1-16.

Lucas CJ, Galettis P, and Schneider J (2018) The pharmacokinetics and the pharmacodynamics of cannabinoids. British Journal of Clinical Pharmacology 84: 2477-2482.

McDougle DR, Kambalya A, Meling DD, and Das A (2014) Endocannabinoids anandamide and 2-arachidonoylglycerol are substrates for human CYP2J2 epoxygenase. Journal of Pharmacology and Experimental Therapeutics 351: 616-627.

Nitta T, Hata M, Gotoh S, Seo Y, Sasaki H, Hashimoto N, Furuse M, and Tsukita S (2003) Size-selective loosening of the blood-brain barrier in claudin-5–deficient mice. The Journal of Cell Biology 161: 653-660.

Pertwee RG (2008) The diverse CB_1 and CB^2 receptor pharmacology of three plant cannabinoids: Δ9-tetrahydrocannabinol, cannabidiol and Δ^9-tetrahydrocannabivarin. British Journal of Pharmacology 153: 199-215.

Pfaffl MW, Tichopad A, Prgomet C, and Neuvians TP (2004) Determination of stable housekeeping genes, differentially regulated target genes and sample integrity: BestKeeper–Excel-based tool using pair-wise correlations. Biotechnology Letters 26: 509-515.

Piomelli D (2015) Neurobiology of Marijuana, in The American Psychiatric Publishing Textbook of Substance Abuse Treatment (5th ed) pp 335-350, American Psychiatric Publishing, Virginia.

Rawitch AB, Rohrer R, and Vardaris RM (1979) Delta-9-tetrahydrocannabinol uptake by adipose tissue: preferential accumulation in gonadal fat organs. General Pharmacology 10: 525-529.

Rubino T and Parolaro D (2016) The impact of exposure to cannabinoids in adolescence: insights from animal models. Biological Psychiatry 79: 578-585.

Sadler NC, Nandhikonda P, Webb-Robertson BJ, Ansong C, Anderson LN, Smith JN, Corley RA, and Wright AT (2016) Hepatic cytochrome P450 activity, abundance, and expression throughout human development. Drug Metabolism and Disposition 44: 984-991.

Sethi PK, White CA, Cummings BS, Hines RN, Muralidhara S, and Bruckner JV (2016) Ontogeny of plasma proteins, albumin and binding of diazepam, cyclosporine, and deltamethrin. Pediatric Research 79: 409-415.

Spear LP (2000) The adolescent brain and age-related behavioral manifestations. Neuroscience and Biobehavioral Reviews 24: 417-463.

Spiro AS, Wong A, Boucher AA, and Arnold JC (2012) Enhanced brain disposition and effects of Δ9-tetrahydrocannabinol in P-glycoprotein and breast cancer resistance protein knockout mice. PLoS One, 7.

Steinberg L (2005) Cognitive and affective development in adolescence. Trends in Cognitive Sciences 9: 69-74.

Stout SM and Cimino NM (2014) Exogenous cannabinoids as substrates, inhibitors, and inducers of human drug metabolizing enzymes: a systematic review. Drug Metabolism Rev. 46: 86-95.

Tapert SF, Schweinsburg AD, and Brown SA (2008) The influence of marijuana use on neurocognitive functioning in adolescents. Current Drug Abuse Reviews 1: 99-111.

Vozella V, Zibardi C, Ahmed F, and Piomelli D (2019) Fast and sensitive quantification of Δ^9-tetrahydrocannabinol and Its main oxidative metabolites by liquid chromatography/tandem mass spectrometry. Cannabis and Cannabinoid Research 4: 110-123.

Wahlqvist M, Nilsson IM, Sandberg F, Agurell S, and Granstrand B (1970) Binding of Δ^1-tetrahydrocannabinol to human plasma proteins. Biochemical Pharmacology 19: 2579-2582.

Watanabe K, Narimatsu S, Matsunaga T, Yamamoto I, and Yoshimura H (1993) A cytochrome P450 isozyme having aldehyde oxygenase activity plays a major role in metabolizing cannabinoids by mouse hepatic microsomes. Biochemical Pharmacology 46: 405-411.

Watanabe K, Yamamoto I, Oguri K, and Yoshimura H (1980) Comparison in mice of pharmacological effects of Δ^8-tetrahydrocannabinol and its metabolites oxidized at 11-position. European Journal of Pharmacology 63: 1-6.

Wiley JL and Burston JJ (2014) Sex differences in Δ^9-tetrahydrocannabinol metabolism and in vivo pharmacology following acute and repeated dosing in adolescent rats. Neuroscience Letters 576: 51-55.

Wong A, Montebello ME, Norberg MM, Rooney K, Lintzeris N, Bruno R, Booth J, Arnold JC, and McGregor IS (2013) Exercise increases plasma THC concentrations in regular cannabis users. Drug and Alcohol Dependence 133: 763-767.

Yin Y, Cao L, Ge H, Duanmu W, Tan L, Yuan J, Tunan C, Li F, Hu R, Gao F, Feng H (2017) L-Borneol induces transient opening of the blood-brain barrier and enhances the therapeutic effect of cisplatin. Neuroreport 28: 506-513.

FOOTNOTES

¶ The study was funded by the National Institute on Drug Abuse (NIDA) [Center of Excellence Grant DA044118]

#This work was supported by the National Institutes of Health [R01 GM1155884]

JPET Fast Forward. Published on April 28, 2020 as DOI: 10.1124/jpet.120.265892
This article has not been copyedited and formatted. The final version may differ from this version.

FIGURE LEGENDS

Fig. 1. Plasma concentrations of Δ^9-THC and its first-pass metabolites, 11-OH-THC and 11-COOH-THC, after IP injection of Δ^9-THC (5, 1.6, 0.5 mg/kg) in adult (A, B, C) or adolescent (D, E, F) mice. Symbols represent mean ± SD, n = 3 or 4 animals per data point, outliers removed using Grubb's test for outliers.

Fig. 2. Brain concentrations of Δ^9-THC, 11-OH-THC and 11-COOH-THC, after IP injection of Δ^9-THC (5, 1.6, 0.5 mg/kg) in adult (A, B, C) or adolescent (D, E, F) mice. Symbols represent mean ± SD, n = 3 or 4 animals per data point, outliers removed using Grubb's test for outliers.

Fig. 3. White adipose tissue (WAT) concentrations of Δ^9-THC, 11-OH-THC and 11-COOH-THC after IP injection of Δ^9-THC (5, 1.6, 0.5 mg/kg) in adult (A, B, C) or adolescent (D, E, F) mice. Symbols represent mean ± SD, n = 3 or 4 animals per data point, outliers removed using Grubb's test for outliers.

Fig. 4. Rate of formation (pmol/min/mg) of 11-COOH-THC (left) and 11-OH-THC (right) in liver microsomes of adult (●) and adolescent (■) mice. Bars represent mean ± SD, $P < 0.05$, n = 4 animals per data point, Student's *t*-test.

Fig. 5. mRNA levels (RQ, Arbitrary Units) of ABC-transporters, *Abcg2* (left), *Abcb1* (center) and claudin-5 (*Cldn-5*, right) in brain of adult (●) and adolescent (■) mice. Bars represent mean ± SD, $P < 0.05$, n = 11 or 12 animals per data point, Student's *t*-test.

JPET Fast Forward. Published on April 28, 2020 as DOI: 10.1124/jpet.120.265892
This article has not been copyedited and formatted. The final version may differ from this version.

Fig. 6. Time-course of the effects of vehicle (saline, 0.9%; ●) or Δ^9-THC (5 mg/kg; ■) administration on motor activity in adult (A) and adolescent (B) mice. Symbols represent mean ± SD, $P < 0.05$, n = 10 per group, two-way ANOVA.

JPET Fast Forward. Published on April 28, 2020 as DOI: 10.1124/jpet.120.265892
This article has not been copyedited and formatted. The final version may differ from this version.

Table 1. Maximal concentration (C_{max}) in plasma, time at which maximal concentration was reached (T_{max}), and half-life of elimination ($t_{1/2}$) for Δ^9-THC and its metabolites in adult and adolescent mice after IP injection of Δ^9-THC (5, 1.6, 0.5 mg/kg). Data are represented as means of n = 4 animals per data point. The standard error of the mean was in all cases >20% and was omitted for clarity. *P < 0.5; **P < 0.01; ***P < 0.001. Student's *t*-test.

Analyte	Dose Δ^9-THC (mg/kg)	Adult				Adolescent			
		C_{max} (pmol/mL)	AUC (pmol•min/mL)	T_{max} (min)	$t_{1/2}$ (min)	C_{max} (pmol/mL)	AUC (pmol•min/mL)	T_{max} (min)	$t_{1/2}$ (min)
Δ^9-THC	5	631	91602	30	109	1111*	86125	15	75*
	1.6	388	32020	15	108	392	18080*	15	88
	0.5	71	9041	15	92	83	6261	15	89
11-OH-THC	5	65	13050	15	123	119***	16087	30	83**
	1.6	22	3675	15	157	21	2572	60	70***
	0.5	6	1391	60	211	8*	676**	30	86
11-COOH-THC	5	260	64731	30	203	654****	126607*	60	159
	1.6	94	19977	30	253	96	20798	60	244
	0.5	25	6104	60	225	41**	7969	30	222

JPET Fast Forward. Published on April 28, 2020 as DOI: 10.1124/jpet.120.265892
This article has not been copyedited and formatted. The final version may differ from this version.

Table 2. Maximal concentration (C_{max}) in brain, time at which maximal concentration was reached (T_{max}), and half-life of elimination ($t_{1/2}$) for Δ^9-THC and its metabolites in adult and adolescent mice after IP injection of Δ^9-THC (5, 1.6, 0.5 mg/kg). Data are represented as means of n = 4 animals per data point. The standard error of the mean was in all cases >20% and was omitted for clarity. *P < 0.5; **P < 0.01; ***P < 0.001. Student's *t*-test.

Analyte	Dose Δ^9-THC (mg/kg)	Adult				Adolescent			
		C_{max} (pmol/g)	AUC (pmol•min/g)	T_{max} (min)	$t_{1/2}$ (min)	C_{max} (pmol/g)	AUC (pmol•min/g)	T_{max} (min)	$t_{1/2}$ (min)
Δ^9-THC	5	1126	261854	120	119	725*	190080	60	134
	1.6	309	75169	60	182	271	56280	60	145
	0.5	97	23044	120	155	85	16693	60	149
11-OH-THC	5	339	71942	120	97	454	82399	60	93
	1.6	83	18582	60	129	140**	19758	60	86**
	0.5	28	6437	60	162	33	4272	30	85*
11-COOH-THC	5	89	21240	120	147	151**	45864*	60	239
	1.6	29	9688	120	284	46*	11946	120	209
	0.5	13	4067	120	296	12	2781	120	198

JPET Fast Forward. Published on April 28, 2020 as DOI: 10.1124/jpet.120.265892
This article has not been copyedited and formatted. The final version may differ from this version.

Table 3. Tissue-to-plasma ratio for Δ^9-THC and its metabolites (11-OH-THC and 11-COOH-THC) in brain or white adipose tissue (WAT) from adolescent and adult mice after IP injection of Δ^9-THC (5 mg/kg). *P < 0.5; **P < 0.01; ***P < 0.001. Student's *t*-test, n = 4 animals per data point.

Analyte	Dose Δ^9-THC	Brain:Plasma		WAT:Plasma	
		Adult	Adolescent	Adult	Adolescent
Δ^9-THC	5 mg/kg	1.9	0.8*	200.9	242.5
11-OH-THC		6.3	3.8*	29.7	19.6*
11-COOH-THC		0.4	0.2**	0.4	0.2***

JPET Fast Forward. Published on April 28, 2020 as DOI: 10.1124/jpet.120.265892
This article has not been copyedited and formatted. The final version may differ from this version.

Table 4. Maximal concentration (C_{max}) in white adipose tissue (WAT), time at which maximal concentration was reached (T_{max}), and half-life of elimination ($t_{1/2}$) for Δ^9-THC and its metabolites in adult and adolescent male mice after IP injection of Δ^9-THC (5, 1.6, 0.5 mg/kg). Data are represented as means of n = 4 animals per data point. The standard error of the mean was in all cases >20% and was omitted for clarity. *P < 0.5; **P < 0.01; ***P < 0.001. Student's *t*-test.

Analyte	Dose Δ^9-THC (mg/kg)	Adult			Adolescent		
		C_{max} (nmol/g)	AUC (nmol•min/g)	T_{max} (min)	C_{max} (nmol/g)	AUC (nmol•min/g)	T_{max} (min)
Δ^9-THC	5	134	55291	30	242*	89246	30
	1.6	51	23509	60	75	29904	30
	0.5	18	6677	120	34	5863	120
11-OH-THC	5	2	323	30	3	336	30
	1.6	0.6	91	60	1*	93	30
	0.5	0.2	25	60	0.1	14*	15
11-COOH-THC	5	0.1	25	120	0.2**	35	60
	1.6	0.03	6	60	0.05*	8	30
	0.5	0.01	3	60	0.01	1*	30

JPET Fast Forward. Published on April 28, 2020 as DOI: 10.1124/jpet.120.265892
This article has not been copyedited and formatted. The final version may differ from this version.

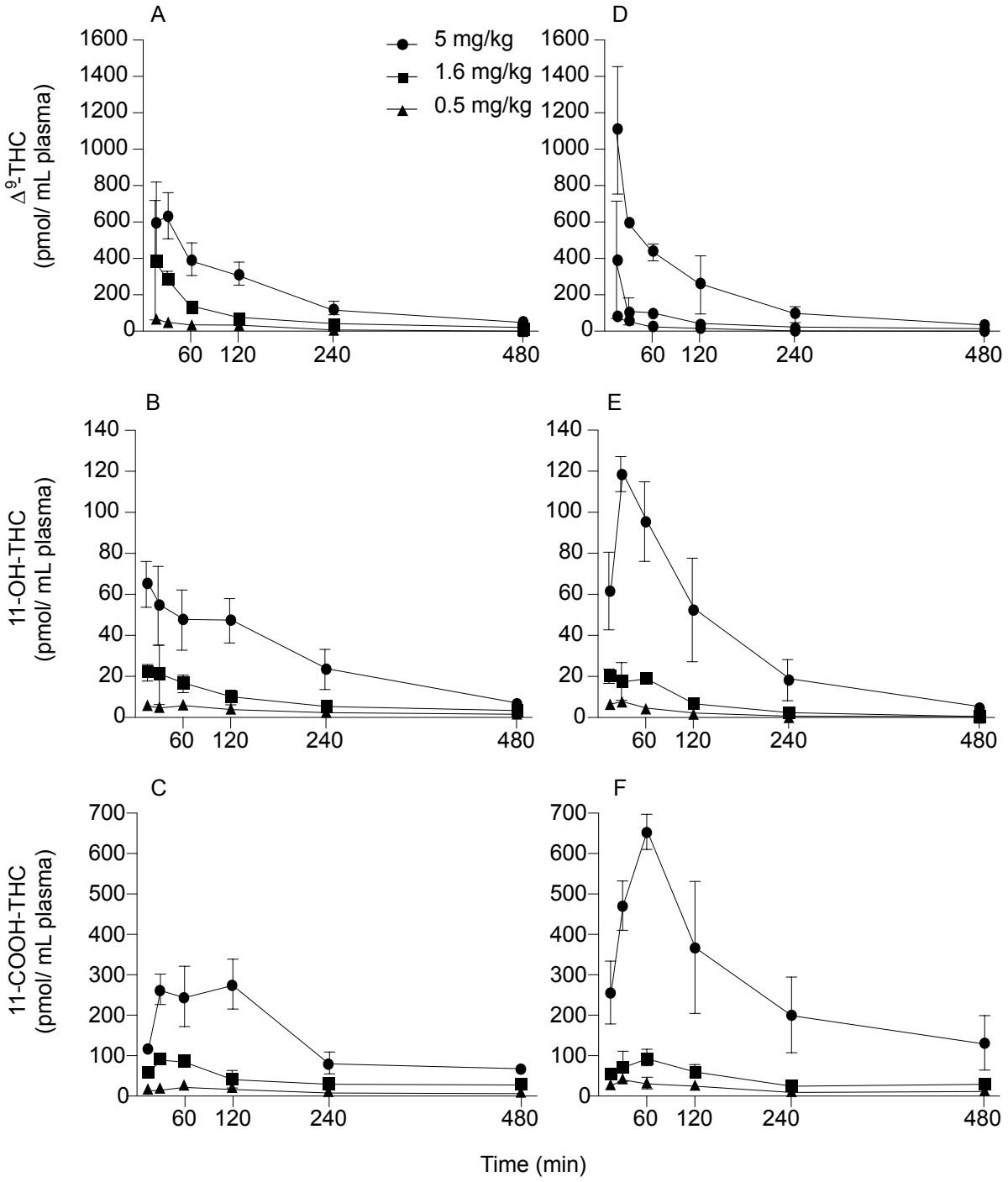

Fig. 1

JPET Fast Forward. Published on April 28, 2020 as DOI: 10.1124/jpet.120.265892
This article has not been copyedited and formatted. The final version may differ from this version.

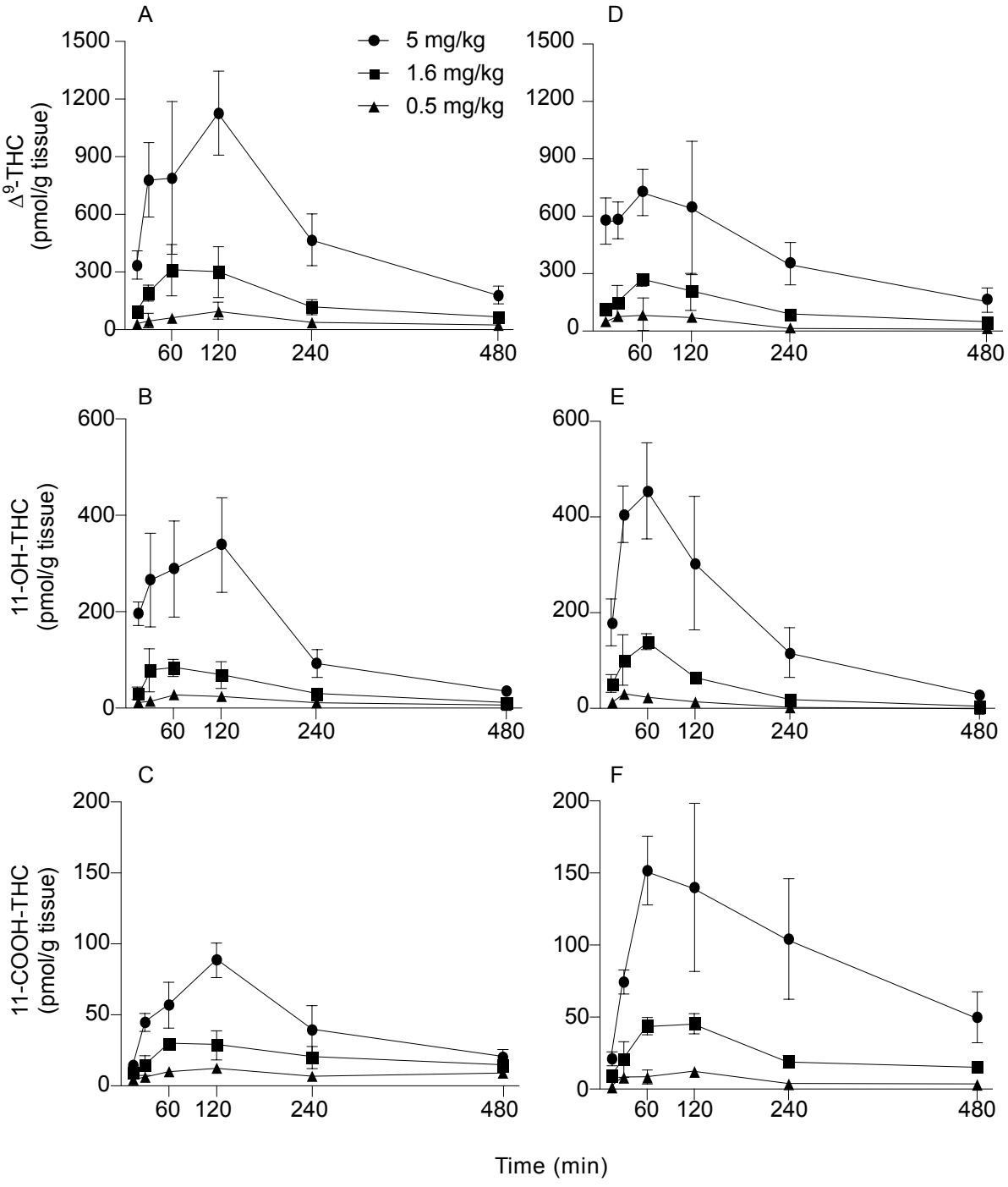

Fig. 2

JPET Fast Forward. Published on April 28, 2020 as DOI: 10.1124/jpet.120.265892
This article has not been copyedited and formatted. The final version may differ from this version.

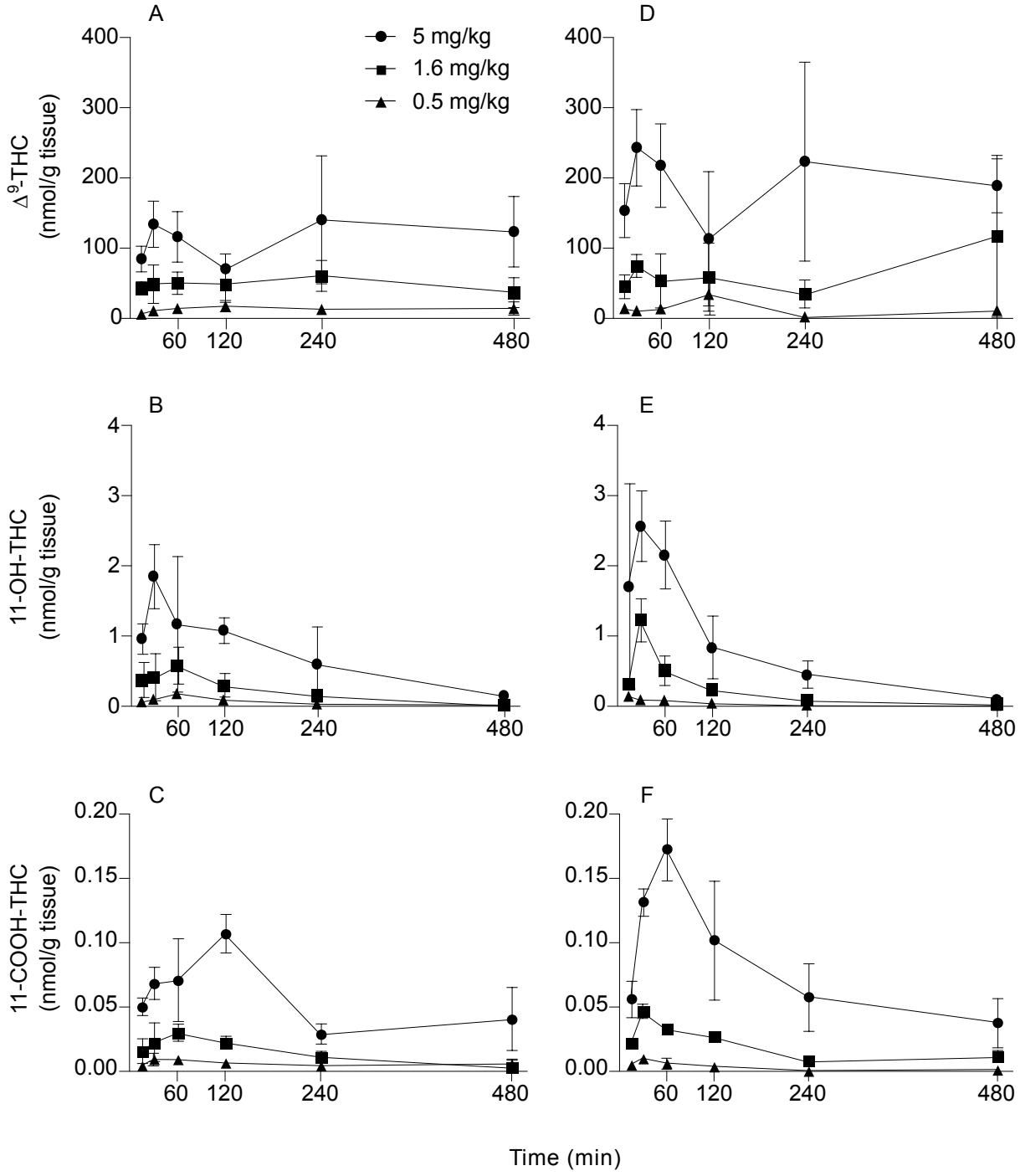

Fig. 3

JPET Fast Forward. Published on April 28, 2020 as DOI: 10.1124/jpet.120.265892
This article has not been copyedited and formatted. The final version may differ from this version.

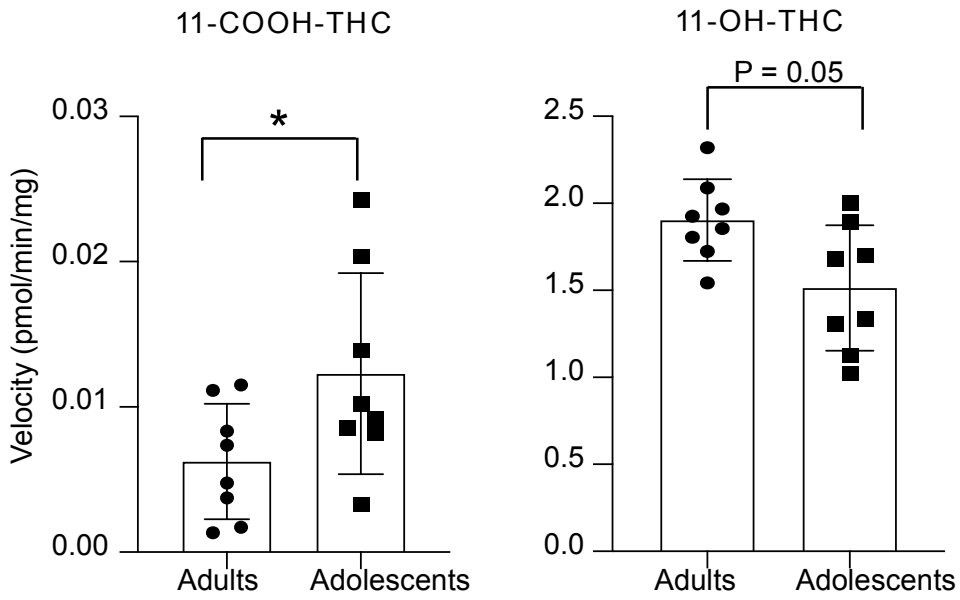

Fig. 4

JPET Fast Forward. Published on April 28, 2020 as DOI: 10.1124/jpet.120.265892
This article has not been copyedited and formatted. The final version may differ from this version.

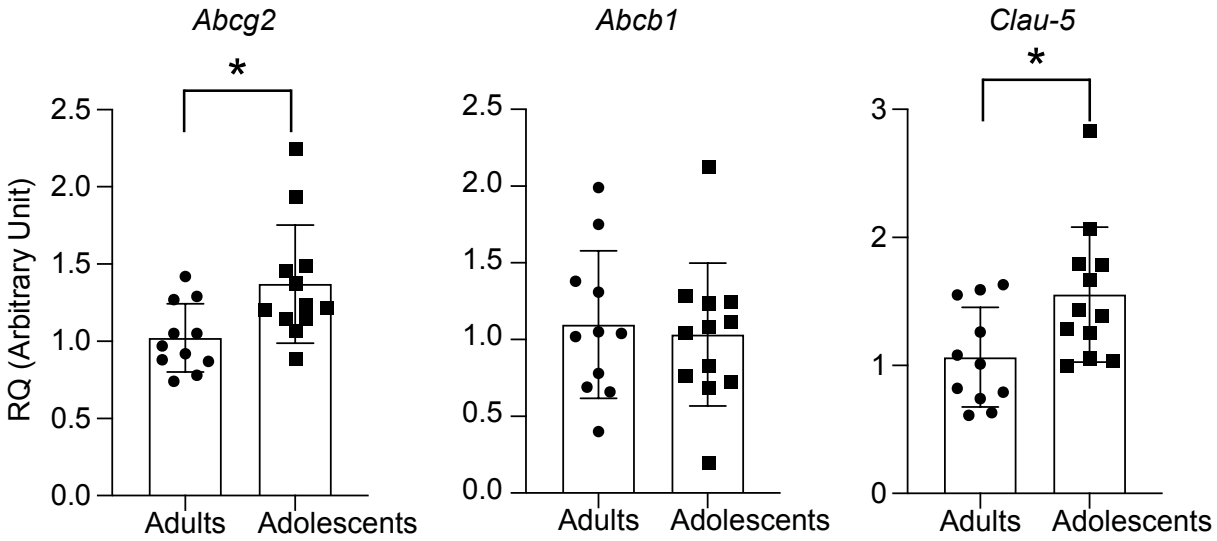

Fig. 5

JPET Fast Forward. Published on April 28, 2020 as DOI: 10.1124/jpet.120.265892
This article has not been copyedited and formatted. The final version may differ from this version.

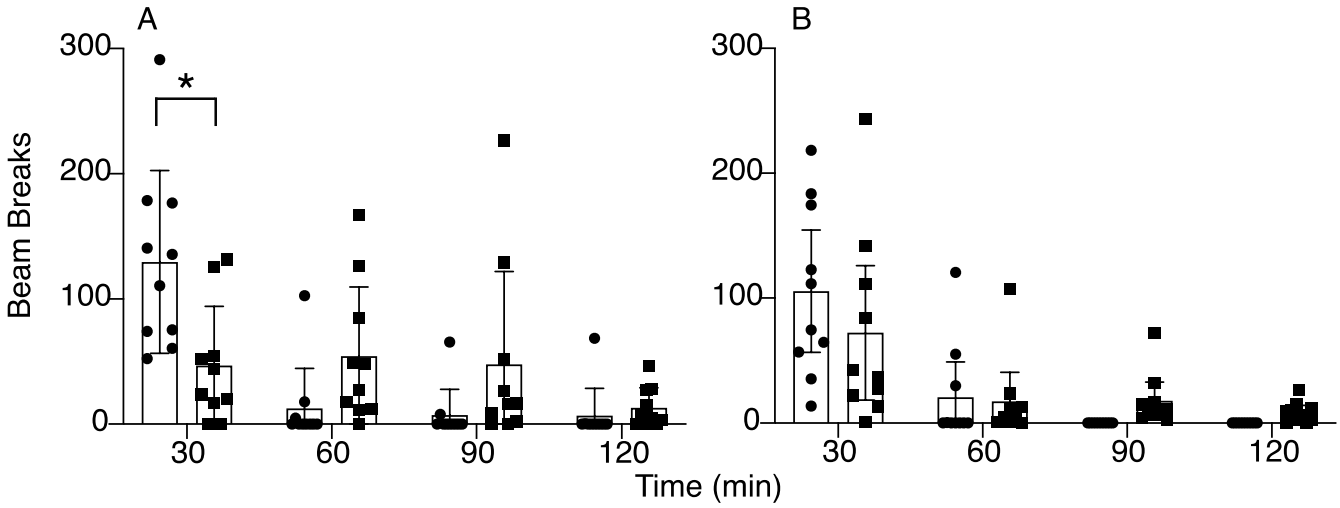

Fig. 6

SUPPLEMENTAL DATA

Comparative Pharmacokinetics of Δ^9-Tetrahydrocannabinol in Adolescent and Adult Male Mice

Alexa Torrens, Valentina Vozella, Hannah Huff, Brandon McNeil, Faizy Ahmed, Andrea Ghidini, Stephen Mahler, Marilyn A. Huestis, Aditi Das, Daniele Piomelli

The Journal of Pharmacological and Experimental Therapeutics

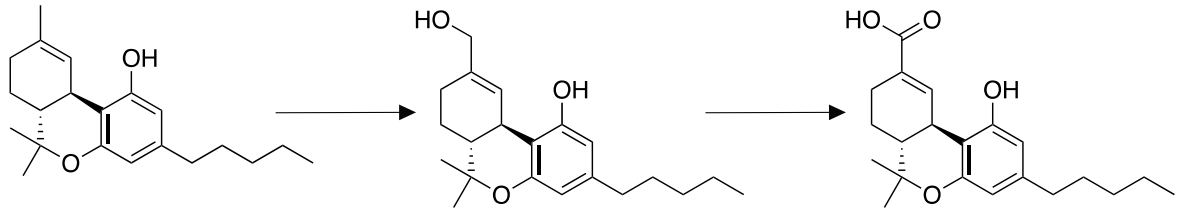

Δ^9-THC
(Active)

11-OH-Δ^9-THC
(Active)

11-nor-9-carboxy-Δ^9-THC
(Inactive)

Supplementary Fig. 1. Cytochrome P_{450}-mediated metabolism of Δ^9-THC. In humans, multiple hepatic and extrahepatic cytochrome P_{450} isoforms (including CYP2C9, CYP2C19 and CYP3A4) convert Δ^9-THC into the biologically active metabolite, 11-hydroxy-Δ^9-THC (11-OH-THC), which is subsequently transformed into the inactive product 11-nor-9-carboxy-Δ^9-THC (11-COOH-THC).

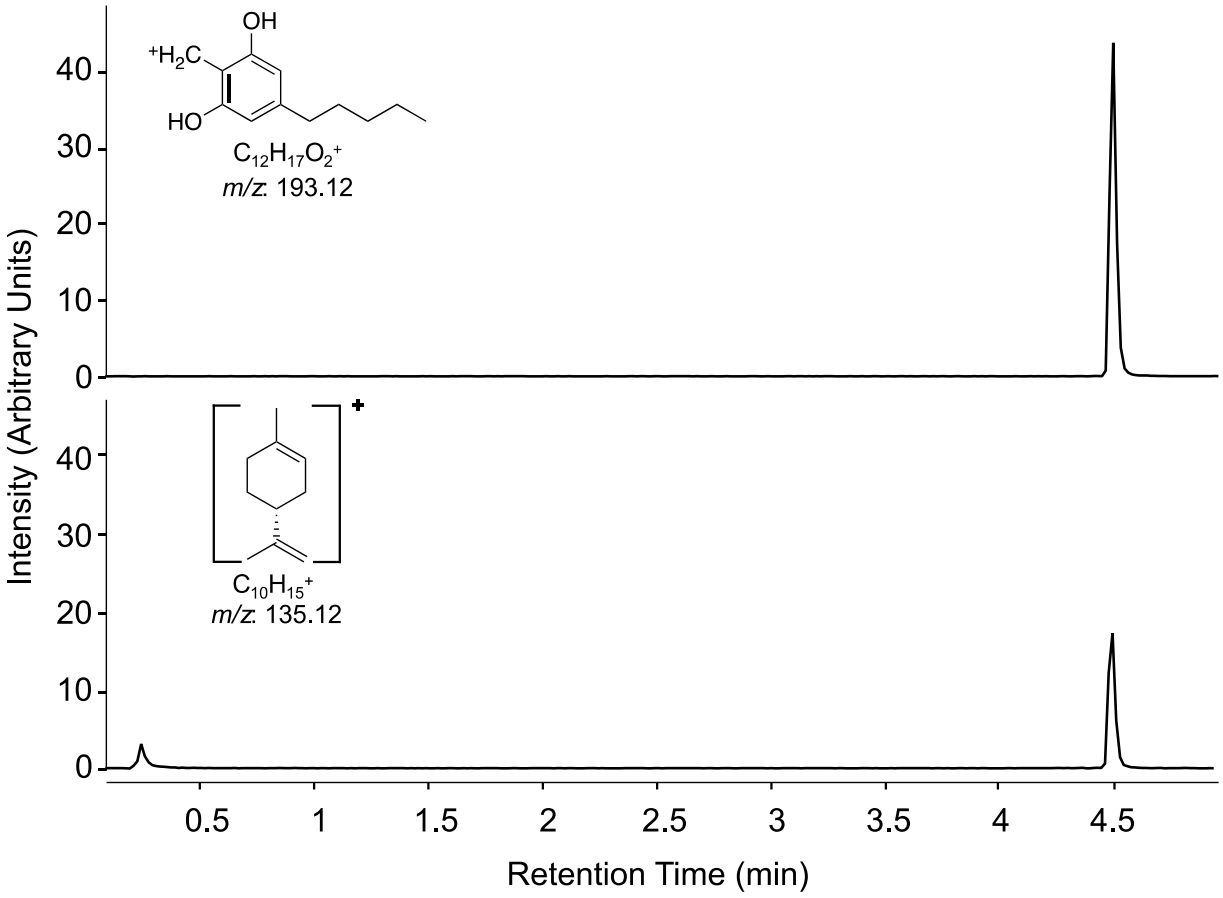

Supplementary Fig. 2. Representative tracing illustrating the LC-MS/MS assay used in the present study for the identification and quantification of Δ^9-THC. The MRM transition 315.2 > 193 *m/z* was monitored for quantification purposes. In select experiments, the MRM transition 315.2 > 135.0 *m/z* was monitored to confirm identity. Authentic standard is omitted for clarity.